Design of a H_2O_2-generating $P450_{SP\alpha}$ fusion protein for high yield fatty acid conversion

Daniele Giuriato[1], Danilo Correddu[1], Gianluca Catucci[1], Giovanna Di Nardo[1], Cristiano Bolchi[2], Marco Pallavicini[2] and Gianfranco Gilardi[1]*

[1]Department of Life Sciences and Systems Biology, University of Torino, Via Accademia Albertina 13, Torino, 10123, Italy.

[2]Dipartimento di Scienze Farmaceutiche Università degli Studi di Milano, Via Mangiagalli 25 I-20133 Milano.

*Corresponding author:

Gianfranco Gilardi

Via Accademia Albertina 13, 10123, Torino, Italy.

Telephone number: +39 011 6704593

Fax number: +39 011 6704643

e-mail: gianfranco.gilardi@unito.it

ABSTRACT

Sphingomonas paucimobilis' $P450_{SP\alpha}$ (CYP152B1) is a good candidate as industrial biocatalyst. This enzyme is able to use hydrogen peroxide as unique cofactor to catalyze the fatty acids conversion to α-hydroxy fatty acids, thus avoiding the use of expensive electron-donor(s) and redox partner(s). Nevertheless, the toxicity of exogenous H_2O_2 toward proteins and cells often results in the failure of the reaction scale-up when it is directly added as co-substrate. In order to bypass this problem, we designed a H_2O_2 self-producing enzyme by fusing the $P450_{SP\alpha}$ to the Monomeric Sarcosine Oxidase (MSOX), as H_2O_2 donor system, in a unique polypeptide chain, obtaining the $P450_{SP\alpha}$-polyG-MSOX fusion protein. The purified $P450_{SP\alpha}$-polyG-MSOX protein displayed high purity (A_{417}/A_{280} = 0.6) and H_2O_2-tolerance (k_{decay}= 0.0021 ± 0.000055 min^{-1}; ΔA_{417}= 0,018 ± 0.001) as well as good thermal stability (T_m: 59.3 ± 0.3 °C and 63.2 ± 0.02 °C for $P450_{SP\alpha}$ and MSOX domains respectively). The data show how the catalytic interplay between the two domains can be finely regulated by using 500 mM sarcosine as sacrificial substrate to generate H_2O_2. Indeed the fusion protein resulted in a high conversion yield toward fat waste biomass-representative fatty acids, i.e lauric acid (TON=6800 compared to the isolated $P450_{SP\alpha}$ TON=2307), myristic acid (TON = 6750) and palmitic acid (TON=1962).

Keywords

$P450_{SP\alpha}$, fatty acids, fusion protein, sarcosine, lanolin.

1. INTRODUCTION

Every year, in European Union alone, the food and textile industry produces more than 200 thousand tons of coarse and low quality shorn wool, which has been estimated to be composed by 15 percent of wool grease, the sheep sebaceous glands exudate, representing an unavoidable sheep farm waste byproduct [1]. Wool grease (also known as lanolin or wool wax) is usually obtained as a raw wool processing derivative, consisting mainly of esters, polyesters of high molecular weight fatty acids and alcohols, along with hydrocarbons and free fatty acids [2]. As previously reported, a possible approach to enhance the value of waste fat biomass is the conversion of lanolin fatty acids to α-hydroxy fatty acids [3]. The hydroxylated products of fatty acids, indeed, find widespread use in chemical, food and cosmetic industry [4] as well as in medical research and medicine [5]. Although the biocatalytic conversion of fatty acids to hydroxy fatty acids has been reported using, among the other, lipoxygenase, hydratase and diol synthase [6], to date the efficient enzymatic production of α-hydroxy fatty acids has not been achieved, leading to the low commercial availability of these compounds. Among all natural and non-natural biocatalysts classes, cytochromes P450 are one of the most versatile in terms of substrate specificity, they are a wide family of hemoproteins nearly ubiquitously distributed among biological kingdoms [7] [8] [9]. The broad variety of chemical reactions catalyzed by this family of enzymes ranges from un-activated carbon hydrogenation, epoxide formation to C-, S-, N- dealkylation, including saturated and unsaturated fatty acids hydroxylation, decarboxylation, and epoxidation in diverse positions [10] [11] [12] [13] [14]. Electrons for these reactions are usually provided by NAD(P)H and transferred to the heme cofactor via different redox partners [15] [16] [17] [18]. Although many P450 are redox partner-dependent monoxygenase, it was

reported that a recently identified sub-family of P450s, named as CYP152, is able to use H_2O_2 as unique source of oxygen and electrons to catalyze the α or β hydroxylation or the oxidative decarboxylation of fatty acids, hence acting as peroxygenases [19] [20] [21] [22]. Indeed, the generally accepted catalytic mechanism of this sub-family of enzymes requires the carboxylic group of the substrate to activate the H_2O_2 and generate the ferryl-oxo cation radical (Compound I), which is responsible for the fatty acid carbon α or β hydrogen abstraction and consequent hydroxylation or decarboxylation [23] [24]. *Sphingomonas paucimobilis* CYP152B1 ($P450_{SP\alpha}$) catalysis is described to exclusively yield the α hydroxylation of fatty acid, exploiting only hydrogen peroxide and not requiring expensive external co-substrate addition or engagement of electron shuttles [25] [26] [27], therefore it is an interesting candidate for applicative exploitation as biocatalyst. Nevertheless, the direct addition of H_2O_2 to the enzyme hampers the modulation of the reaction and the stability of the system, resulting in poor regulation of the catalysis and, ultimately leading to the failure of reaction scale-up [28]. In order to bypass the complication of direct use of H_2O_2, diverse strategies that aim to control the *in situ* H_2O_2 supply have been reported to promote peroxygenases catalysis, including the development of self-sufficient chimeric fusion enzymes [29] [30]. In line with the Molecular Lego approach developed in our laboratory [31] [32], where proteins with different functions are fused in chimeras where the resulting continuous polypeptide chain gains a combined catalytic properties for specific purposes, in this work we present a CYP152B1 H_2O_2 self-producing enzyme, fusing the $P450_{SP\alpha}$ to the Monomeric Sarcosine Oxidase (MSOX), as H_2O_2 donor system, in a unique polypeptide chain. Monomeric Sarcosine Oxidase from *Bacillus sp. B-0618* is an extensively studied bacterial flavin-bound oxidoreductase [33] [34] [35] [36] [37]. It is a member of a family of

prokaryotic and eukaryotic enzymes containing covalently bound flavin, which generally catalyse the oxidative dealkylation of various N mono- or di- substituted amino acids substrates to the corresponding native amino acids, with the concomitant reduction of molecular oxygen to hydrogen peroxide. The main reaction catalysed by MSOX is the oxidative demethylation of sarcosine (N-methylglycine) to yield glycine, formaldehyde, and hydrogen peroxide as by-product. In this work we rationalized the development of the fusion protein aiming to exploit the MSOX by-product H_2O_2 (1) to drive the $P450_{SP\alpha}$ fatty acid hydroxylation (2):

$$CH_3N^+H_2CH_2COO^- + O_2 + H_2O \rightarrow N^+H_3CH_2COO^- + HCHO + H_2O_2 \quad (1)$$

$$CH_3(CH_2)_nCH_2COO^- + H_2O_2 \rightarrow CH_3(CH_2)_nCHOHCOO^- + H_2O \quad (2)$$

Moreover, we focused on the modulation of MSOX catalysis working on sarcosine concentration employed to provide the optimal amount of H_2O_2 needed for the P450 catalysis over the entire reaction time course. Finally, we exploited the H_2O_2- generating $P450_{SP\alpha}$ fusion protein system to convert three fatty acids notoriously present in lanolin, i.e. lauric acid, myristic acid and palmitic acid, [38] [39] to the corresponding α-hydroxy fatty acids.

2. RESULTS

2.1 Fusion protein design, expression and purification

In order to obtain a catalytically self-sufficient form of the $P450_{Sp\alpha}$, we designed a fusion protein in which the CYP domain is structurally fused to the H_2O_2-donor domain MSOX. The two enzymes are joined by a linker loop, composed by eleven amino acids, i.e. Gly-Pro-$(Gly)_7$-Pro-Gly. The poly glycine sequence was chosen because of the low steric hindrance of the glycine residues, indeed the linker is intended to allow the highest possible flexibility of the

loop connecting the two domains to support conformational rearrangements and avoid misfolding of the fusion protein. The SPα-SOX designed gene has been sub-cloned into a $KanR^+$ pET-28-a(+) expression vector exploiting the NcoI/EcoRI cloning system. Expression was carried out in BL21 (DE3) *E. coli* strain as host cells to maximize the protein expression yield. Kanamycin was used to set the selective pressure needed to advantage the growth of pET-28-a(+) kanamycin resistant transformed cells. Protein purification was performed using immobilized metal affinity chromatography (IMAC), exploiting the engineered protein C-terminal 6xHis-tag affinity toward nickel ions. Protein expression in *E. coli* was found to yield both full length protein and a truncated form likely due to the bacteria endogenous protease activity, corresponding to the C-terminal MSOX domain. Since the C-terminal 6xHis-tag is present in both the full-length and truncated protein form, adequate purity of the full-length fusion protein cannot be achieved using only IMAC. For this reason, the IMAC was followed by a size exclusion chromatography. The two-step purification led to a protein batch showing a major single band at about 90 kilodaltons on SDS-PAGE (Fig. 2A), consistent with the predicted SPα-SOX molecular mass of 91.6 kilodaltons (His-tag included). The fusion enzyme purity was found to be around 0.6, expressed as the ratio between the absorbance maxima at λ_{417} and λ_{280}.

2.2 Spectroscopic characterization

The UV-visible properties of SPα-SOX fusion protein were characterized for both the heme (CYP152B1) and flavin (MSOX) domain by absorbance spectroscopy. The absorbance spectrum of the fusion protein showed a Soret absorption peak at 417 nm and other maxima around 353, 535, 574 nm., as expected for the six-coordinate low-spin state ferric heme of

$P450_{Spα}$ [25]. The characteristic flavoprotein absorption bands with maxima at 372, 454 ($ε_{454nm}$: 12 200 M^{-1} cm^{-1}) and a shoulder at 475 nm, was also observed [34] (Fig. 2B, 2C). The spectral features are consistent with the oxidized state of the CYP152B1 and MSOX domains [25 35]. The reduction of the protein with sodium dithionite produced a decrease of the $P450_{Spα}$ 417 nm absorbance band ($Fe^{III} \rightarrow Fe^{II}$) [40] (Fig. 2B). Concomitantly it was observed the decrease of the 454 and 475 nm bands, likely due to the MSOX reduction [36]. After that, the protein sample was bubbled with carbon monoxide, resulting in the Soret peak conversion to 445 nm, due to Fe^{II}-CO complex formation (Fig. 2B). This Soret feature, slightly different compared to the typical P450 CO-complex absorbance peak at 450 nm, was already reported for $P450_{Spα}$ and other CYP152 family members [25 41 42 27]. The MSOX domain integrity was investigated by monitoring the UV-VIS spectral change of the SPα-SOX fusion enzyme before and after the addition of sarcosine (Fig. 2C). Similarly to the free FAD, MSOX is known to undergo specific spectral changes when reduced through two-electron transfer, i.e. the complete bleaching of the oxidized enzyme spectrum [36]. In our study, the spectroscopic behavior of the flavin cofactor upon reduction with sarcosine is detected within the fusion protein spectrum (Fig. 2C). Immediately after sarcosine addition, a decrease in absorbance at $λ_{372}$ and $λ_{454}$ was observed, in line with the conversion of the oxidized MSOX flavin to the two-electron reduced form [36].

2.3 Thermal denaturation

In order to investigate the enzyme unfolding process and define the melting temperature of the two domains within the context of the fusion protein system, we analyzed the thermal denaturation of SPα-SOX using the differential scanning calorimetry. The fusion protein was denatured by increasing the temperature between 25°C and 90°C at a scan/rate of 60°C/hr and

experimental thermogram was accurately fitted (Fig. 3A). The result of the fitting was then deconvoluted to obtain the protein single domains denaturation endothermal peaks (Fig. 3B). Overall the SPα-SOX displays a relatively high energy barrier to denaturation, with a measured temperature of melting (T_m) of 59.3 ± 0.3 °C and 63.2 ± 0.02 °C for the two domain respectively (Fig. 3B). The reported T_m of native sarcosine oxidase is 64.0 °C [43 44], in line with our data, for this reason we assigned the first endothermal peak of the thermogram to $P450_{Spα}$ domain (T_m: 59.3 °C) and the second endothermal peak to MSOX domain (T_m: 63.2 °C) (Fig. 3B). To our knowledge, the melting temperature of $P450_{Spα}$ hasn't been reported yet.

2.4 Hydrogen peroxide tolerance

The toxicity of oxidative stress toward proteins and cells is known [28]. In the case of P450s, H_2O_2 causes oxidative damage to the protein and to the iron protoporphyrin, usually leading to the oxidation of the heme thiolate ligand to sulfenic acid [45], this causes a decrease in heme absorbance Soret band [46] and a loss of P450 catalytic performance. Indeed the overall aim of our work is to obtain a catalytically self-sufficient peroxygenase, therefore the $P450_{Spα}$ stability to hydrogen peroxide in the fusion protein system is a crucial point in order to achieve our purpose. The hydrogen peroxide tolerance of the SPα-SOX heme domain in presence of 1 mM H_2O_2 was assessed by taking UV-VIS spectra of the protein over one hour of incubation and monitoring the A_{417} decreasing (Fig. 3C). The SPα-SOX stability was expressed through the heme Soret peak decay rate constant (k) and the amplitude of A_{417} decrease. The decay rate constant (k) of the Soret peak is a quantitative measure of the heme thiolate ligand oxidation kinetics and it gives information about the enzyme stability in presence of H_2O_2. Hydrogen peroxide tolerance data were compared in Table 1 with those previously obtained for: $OleT_{JE}$

(CYP152L1), fatty acid hydroxylases P450 BM3, P450 monoxygenases CYP51B1, CYP121A1 and CYP116B5 [46] [47]. As shown in Table 1, $P450_{Spα}$ in the fusion protein system shows both a lower decay rate constant (k= 0.0021 ± 0.000055 min^{-1}) and a lower amplitude of A_{417} decrease (A= 0.018 ± 0.001) compared to the other reference enzymes, as expected by the peroxygenase function [46] [47]. Notably, the stability toward hydrogen peroxide of the SPα-SOX is higher compared to the CYP152 peroxygenase family member $OleT_{JE}$ (k= 6.99 ± 0.16; A= 0.065 ± 0.001)[46].

2.5 Fatty acids conversion

In order to investigate the SPα-SOX catalysis, three fatty acid, i.e. lauric acid, myristic acid and palmitic acid, were chosen as $P450_{SPα}$ representative substrates. The optimal concentration of sarcosine to drive the reaction was identified measuring the percentage of palmitic acid conversion over time during 4 h of incubation with an increasing concentration of sarcosine. Palmitic acid is the $P450_{SPα}$ substrate with the higher turnover rate among those used in our work [26], it is therefore a good marker substrate to define the most advantageous sarcosine concentration to drive the system catalysis. For all the sarcosine concentration used, SPα-SOX catalyzed the palmitic acid conversion and for each of them the conversion time course is reported in Fig. 4. The system shows an increase in the rate of substrate consumption with a sarcosine concentration ranging between 25 and 500 mM. Further increase of sarcosine concentration up to 1 M leads to a decrease in the conversion rate, attributable to the toxic effect due to the excess of H_2O_2 (Fig. 4). 500 mM sarcosine was used for all the other experiments involving the SPα-SOX self-sufficient for the lanoline-representative fatty acids conversion tests (Table 2). Fig. 5 shows representative GC traces of the sarcosine-driven SPα-

SOX conversion of lauric acid, myristic acid and palmitic acid. $P450_{SP\alpha}$ is known to convert fatty acids to α-hydroxy products with a specific yield of at least 94.6 % [23]. In our experiments the SPα-SOX catalysis led to the detection of one product for each lanoline-representative fatty acid, with a conversion yield up to 100 % (Table 2, Fig. 5). The incubation of each fatty acid with H_2O_2 did not result in α-hydroxy products, confirming that the $P450_{SP\alpha}$-mediated H_2O_2 activation is required for the production of α-hydroxy fatty acids. The SPα-SOX catalytic performance, in terms of percentage of substrate consumption and TON, when the sarcosine-driven H_2O_2-generating system is exploited, was found to be overall higher or comparable to that obtained by the direct addition of H_2O_2, with the exception of the condition with the highest concentrations palmitic acid (5 and 10 mM, Table 2). Comparing the two H_2O_2 supply method, it was observed that the sarcosine-driven catalysis was lower when a higher concentrations palmitic acid is used. This effect could be due to the MSOX instability in presence of a high concentration of the fatty acid. Of note, the SPα-SOX system, regardless the H_2O_2 supply method used, shows a higher percentage of conversion for all the lauric acid concentration tested compared to the isolated $P450_{SP\alpha}$ (Jiang et al. [23]), specifically the conversion yield of SPα-SOX increased by 36.6, 46.6, 18.8 and 50.5 % using 0.5, 1, 5 and 10 mM lauric acid when the fusion protein catalysis is driven by a stochiometric concentration of H_2O_2, i.e. the same conditions used by Jiang et al. for the $P450_{SP\alpha}$ experiment (Table 2) [23]. On the other hand, using 500 mM of sarcosine to drive the fusion enzyme self-sufficient catalysis, the conversion yield of SPα-SOX is higher compared to the isolated $P450_{SP\alpha}$, but comparable with the SPα-SOX system driven by exogenous H_2O_2 (Table 2). Sarcosine-driven self-sufficient SPα-SOX system increased the myristic acid conversion yield compared to the direct H_2O_2 supply method.

Indeed it was found that using sarcosine to induce the fusion enzyme catalysis, the overall conversion increased by 43.8, 21.6, 7.4 and 31.9 % using 0.5, 1, 5 and 10 mM substrate respectively compared to the H_2O_2 directly induced catalysis. The enzyme reached the highest turnover number using 10 mM of myristic acid (6750 μM myristic acid converted using 1 μM enzyme sustained by 500 mM sarcosine), in line with a better regulation of the H_2O_2 production, achieved by exploiting MSOX as H_2O_2-generating system.

2.6 Catalytic interplay between the two domains

Aiming to investigate the underlying reason for the enhanced activity of the fusion protein system, we measured the hydrogen peroxide accumulated in the reaction medium during the self-sufficient catalysis of SPα-SOX. In order to investigate the efficiency of H_2O_2 consumption of SPα-SOX, we monitored the amount of H_2O_2 in presence of a stoichiometric concentration of lauric acid ranging from 0.5 to 10 mM in a time course experiment. Fig. 6A shows that SPα-SOX consumed up to 5 mM of H_2O_2 in less than 30 minutes and up to 10 mM in about 60 minutes. We thus investigate the effect of the fatty acids concentration to SPα-SOX self-sufficient catalysis, monitoring the sarcosine-driven H_2O_2 concentration in solution at increasing concentration of lauric acid. Fig. 6B shows the accumulation trend of H_2O_2 produced by MSOX domain induced by 500 mM sarcosine at different lauric acid concentrations. Data shows that the time course of H_2O_2 accumulation in solution depends on the lauric acid concentration, indicating that the substrate conversion can be directly correlated to the H_2O_2 consumption (Fig. 6B).

3. DISCUSSION

In this study, we present the design, production, characterization and catalytic performances of an engineered SPα-SOX fusion enzyme. In the catalytically self-sufficient system MSOX produces H_2O_2 as a byproduct from the oxidation of sarcosine as substrate. The $P450_{SP\alpha}$ acts as catalytic domain of the system, consuming the H_2O_2 to drive the α-hydroxylation of fatty acids commonly present in lanolin i.e. lauric acid, myristic acid, and palmitic acid [38] [39]. The formation of the P450 CO-complex, leading to the complete red-shift of the $P450_{SP\alpha}$ Soret absorption peak (Fig. 2B) confirms that the heme domain of the fusion protein maintained a good folding state during the expression and the purification, and that the heme cofactor is well buried inside the $P450_{Sp\alpha}$ catalytic pocket structure [48]. According to the accepted reaction mechanism of MSOX, the covalently bound flavin cofactor (8R-*S*-cysteinyl-FAD) of the enzyme is converted to the two electron reduced form right after the mixing with sarcosine [36], leading to the complete bleaching of the oxidized enzyme spectrum, as observed for SPα-SOX spectral chance upon addition of sarcosine (Fig.2C). Overall, the spectroscopic characterization of the fusion enzyme confirm correct cofactors incorporation and reactivity. If the two SPα-SOX domains are compared in terms of unfolding behaviour (Fig. 3B), the peak associated to MSOX domain results in a more cooperative transition and a higher energy barrier to unfolding, indicating a contribution of the MSOX domain in stabilizing the fusion protein in solution, as previously observed for other P450 fusion proteins [49]. This is the first time that the $P450_{Sp\alpha}$ H_2O_2 tolerance is investigated spectrophotometrically, whereas the higher stability toward H_2O_2 of $P450_{Sp\alpha}$ compared to $OleT_{JE}$ and other CYP152 peroxygenases has been already studied in terms of residual activity of the enzyme in presence of H_2O_2 by Jiang et al. and reported in [23]. Indeed, previous data showed that the residual activity of $OleT_{JE}$ for the

conversion of lauric acid, cis-2-dodecenoic acid and trans-2-dodecenoic acid, in presence of 2 mM H_2O_2 is nullified by enzyme inactivation, whereas $P450_{Spα}$ can still maintain high catalytic activity in presence of H_2O_2 up to 10 mM with a good conversion yield (23.1 %) [23]. These data support our observations about the lower decay rate and the lower overall protein loss of the SPα-SOX system compared to the $OleT_{JE}$ peroxygenase [46] (Table 1). Unexpectedly, the results of our SPα-SOX catalysis experiment indicate that even without exploiting the MSOX as H_2O_2-generating system, thus by directly adding exogenous H_2O_2 in solution, the $P450_{SPα}$ catalytic performance for the conversion of lauric acid in the fusion protein context is enhanced compared to the isolated enzyme [23], a similar result was obtained by exploiting the sarcosine-driven system (Table 2). Although further investigation is needed to clarify the underlying mechanism, the proximity to the highly soluble MSOX domain may stabilize the $P450_{SPα}$ structure in solution, resulting in a more catalytically efficient system compared to the isolated enzyme, regardless the H_2O_2 supply method used. The sarcosine-driven self-sufficient SPα-SOX system increased the myristic acid conversion yield compared to the direct H_2O_2 supply method (Table 2). The high turnover of $P450_{SPα}$ toward myristic acid was already reported and has been correlated with the prevalent presence of myristic acid in the sphingoglycolipids composition of the $P450_{SPα}$ origin organism *Sphingomonas paucimobilis* [27 50]. In any case, this data is in line with a better regulation of the H_2O_2 production, achieved by exploiting MSOX as H_2O_2-generating system. By measuring the hydrogen peroxide accumulated in the reaction medium during the self-sufficient catalysis of SPα-SOX, we aimed the underlying reason for the enhanced activity of the fusion protein system. By evaluating the time course of H_2O_2 it can be observed that the H_2O_2 accumulation in solution depends on the lauric acid

concentration, indicating that the substrate conversion can be directly correlated to the H_2O_2 consumption (Fig. 6B). This is fully in line with the results reported in Table 2 where an increasing TON is found at higher substrate concentrations.

4. CONCLUSION AND OUTLOOK

Sphingomonas paucimobilis' $P450_{SP\alpha}$ is able to use hydrogen peroxide as unique cofactor to convert fatty acids yielding high value α-hydroxy fatty acids [25] [26] [27]. Nevertheless, the toxicity of H_2O_2 toward protein and cells usually results in the failure of the reaction scale-up [28]. Attempts have been made to avoid the direct use of H_2O_2 to drive the peroxygenases catalysis by exploiting indipendent protein H_2O_2-donor enzyme such as the AldO/glycerol system [23] or fusion proteins [46]. The approach of engineering P450 fusion proteins to obtain catalytically self-sufficient enzymes has shown excellent results [51] [31] [52]. In this work we rationalized the development of the SPα-SOX fusion enzyme aiming to exploit the MSOX by-product H_2O_2 to drive the $P450_{SP\alpha}$ fatty acid conversion. Our data suggest that the regulation of the interplay between the two SPα-SOX fusion enzyme domains is achievable by fine-tuning the MSOX and $P450_{SP\alpha}$ substrates concentration, therefore acting respectively on the rate of production and consumption of the catalytic intermediate H_2O_2. This leads to the optimal amount of hydrogen peroxide in solution necessary for $P450_{SP\alpha}$ catalysis and stability. The mechanism of action of the SPα-SOX needs to be further investigated, particularly for what concerns the inter-domain interaction and the mutual effect of the physical proximity of $P450_{SP\alpha}$ and MSOX on their catalysis. It was reported that a high concentration of sarcosine (also known as an important organic osmolyte) increases the thermodynamic stability of folded proteins such as RNAse A and egg white lysozyme, resulting in significant increase in the thermal unfolding

transition temperature (T_m) for these proteins [53] [54]. The investigation of the effect of the high concentration of sarcosine to our fusion protein system stability could be helpful to understand the underlying mechanism of the high catalytic performance of the self-sufficient SPα-SOX.

5. MATERIALS AND METHODS

5.1 Chemicals

All solvents and reagents were of analytical grade and were obtained from Sigma Aldrich (MO, USA).

5.2 P450$_{SPα}$-polyG-MSOX gene design and plasmid vector construction

The gene of P450$_{SPα}$-polyG-MSOX (SPα-SOX) was designed by fusing the coding sequence of CYP152B1 from *Sphingomonas paucimobilis* [27] and the Monomeric Sarcosine Oxidase gene from *Bacillus sp. B-0618* [33]. The two enzyme genes are linked through 33 bp (3) sequence coding for a poly-glycine linker, inserted between heme domain and sarcosine oxidase (Fig. 1). The linker is flanked by AvrII and AscI restriction sites respectively at 5' and 3' of the linker sequence (Fig. 1C). 6 CAC triplets, coding for 6xHis-tag, were inserted in-frame between MSOX last codon 3' and TAA stop codon, as the C-terminal His-Tag can be exploited for protein purification. The designed gene results in 2496 bp.

GGTCCAGGTGGCGGCGGTGGTGGCGGCCCAGGT (3)

The SPα-SOX gene insertion and plasmid construction were performed by GenScript (Piscataway, NJ, USA). The first codon of the CYP152B1 sequence is preceded by a ATG triplet, which defines the open reading frame of the gene. The resulting protein consists in the

CYP152B1 as N-terminal domain, followed by the linker and Monomeric Sarcosine Oxidase as C-terminal domain. The protein linker, translated with CYP152B1 domain reading frame, results in 11 amino acids sequence: Gly-Pro-$(Gly)_7$-Pro-Gly. The SPα-SOX gene was cloned in a pET-28-a(+) NcoI/EcoRI-digested expression vector, resulting in a 7751 bp circular DNA strand. The pET-28-a(+) harbors a KanR gene, conferring resistance to Kanamycin when expressed in bacteria and a Lac-I operon inducible by IPTG.

5.3 Protein expression and purification

The pET plasmid, harboring the SPα-SOX gene (C-terminal 6xHis-Tag), was used to transform *E. coli* BL21 (DE3) cells by heat shock. The transformed bacteria were grown at 37° C in Terrific broth (TB) medium and selected with 50 μg/ml Kanamycin. After the optical density at 600 nm reached 0.4 - 0.6, the culture temperature was lowered to 20° C, 0.5 mM δ-aminolevulinic acid and 50 μg/ml riboflavin was added. The expression was induced by adding 0.125 mM IPTG and carried out for 24 h at 20°C. The cells were harvested by centrifugation at 4° C, resuspended and sonicated (5 × 30 s pulses with a Misonix Ultrasonic Sonicator, Teltow, Germany) in 50 mM KPI at pH 7.4 supplemented with 100 mM KCl, 1% Triton X-100, 20 mM imidazole, 1 mg/ml lysozyme, 0.1 mg/ml DNAse I, 1,5 mM PMSF and 1 tablet/50 ml cOmplete protease inhibitor (Roche). After 45 minutes ultracentrifugation at 40000 rpm, the soluble fraction of cell lysate was loaded into 5 ml nickel-ion affinity column (His-trap HP, GE Healthcare) hold at 8° C. The column was washed with 50 mM KPI at pH 7.4 supplemented with 20 mM imidazole and then with 100 mM imidazole. The target bounded protein was eluted isocratically with 300 mM imidazole. The nickel-ion affinity column eluate was loaded into size exclusion chromatography (HiLoad 16/600 Superdex 200 pg) in 50 mM KPi pH 7.4, 500

mM KCl. The purified protein was stored at -20° C in 50 mM KPi pH 7.4, 200 mM KCl, 20% glycerol. Protein purity was assessed by SDS-PAGE. After reduction with sodium dithionite and pure carbon monoxide bubbling, the spectrum of the $P450_{SP\alpha}$ Fe^{II}-CO form was used to evaluate the concentration of the active folded protein, using an ε_{445nm} of 91000 M^{-1} cm^{-1} [55]. The reduction of MSOX domain was evaluated by detecting the UV-VIS spectral change of 2.4 μM of the purified enzyme before and after the addition of 11.2 mM of sarcosine.

5.4 Differential scanning calorimetry

DSC was performed using a Microcal VP-DSC instrument (Malvern). The experimental data were analyzed using Microcal Origin software. All protein samples were analyzed applying a temperature gradient of 25–90 °C with a scan rate of 60 °C/h, after 10 min of pre-scan equilibration [51 56 57]. In order to provide the best protein stability condition, sample were suspended in 50 mM KPI at pH 7.4, 10 % glycerol, 100 mM KCl, the same buffer was used also for reference scans. All samples were run using 5 μM enzyme.

5.5 Spectroscopic estimation of hydrogen peroxide tolerance

P450 tolerance to H_2O_2 was investigated using Agilent 8453 UV–vis spectrophotometer and monitoring the SPα-SOX UV-VIS spectra maximum at λ_{417} over 60 minutes of incubation at 10 ° C (Peltier Agilent 89,090 A) with H_2O_2. 1.7 μM of enzyme was incubated in KPI 50 mM at pH 7.4 and 1 mM of H_2O_2. Spectra were recorded every 1.5 minutes. A_{417} was plotted against time and data were fitted using a single exponential decay function to obtain the decay rate constant (k).

5.6 Enzyme catalysis assays

Fatty acids conversion reactions were carried out at 30 °C in a 50 mM KPI buffer at pH 7.4 supplemented with 5% ethanol as co-solvent. All the reaction were started by the addition of the reducing agent (sarcosine or H_2O_2). For the identification of the optimal sarcosine concentration 1 μM SPα-SOX and 1 mM palmitic acid were mixed with 25, 250, 500 or 1000 mM sarcosine, identical mixtures were prepared without the enzyme and used to estimate the untreated palmitic acid concentration. Aliquots of reaction and untreated substrate mixtures were collected 1, 2 or 4 hours after the reaction start to monitor the palmitic acid conversion over time. For the overall fatty acids conversion analysis, 1 μM SPα-SOX was incubated for 6 hours with 0.5, 1, 5 or 10 mM substrate (lauric acid, myristic acid or palmitic acid) and, respectively, 0.5, 1, 5 or 10 mM H_2O_2 or 500 mM sarcosine, identical mixtures were prepared without the enzyme and used to estimate the untreated palmitic acid concentration. All the samples were extracted, derivatized and analyzed by gas chromatography (see section 5.7), the percentage of conversion was calculated by comparing the reactions to the untreated substrate mixtures.

5.7 Gas chromatography separations

Fatty acids containing samples were analyzed using a Agilent 7890A gas chromatograph equipped with a capillary column (HP-5 5% Phenyl Methyl Siloxan: Agilent 19091J-413, 320 μm diameter, 30 m length, 0.25 μm film thickness). The oven program was set at 70 °C for 2 min then 15 °C/min to 300 °C for 5 min. The injection volume was 2.5 μL. All fatty acids conversion reaction samples were carried out in 500 μL KPI 50 mM pH 7.4 and extracted, at

the due time, with 500 µL methyl tert-butyl ether (MTBE). Extracted samples were dried using magnesium sulfate ($MgSO_4^-$) and derivatized adding 25 % v/v N,O-Bis(trimethylsilyl)-trifluoroacetamide with trimethylchlorosilane and incubating for 1 hour at 50° C.

5.8 Hydrogen peroxide quantification

In order to investigate the catalytic interplay between the two domains of SPα-SOX, the horseradish peroxidase (HPR) was used to quantify the H_2O_2 produced by MSOX and consumed by the $P450_{SPα}$. A calibration curve was obtained by mixing 0.5 µM Horseradish peroxidase (HPR), 250 µM ABTS and either 1, 2, 10, 15, 20, 30, 40, 50 or 100 µM H_2O_2, after 10 minute incubation in 50 mM KPI at pH 7.4, at 30° C the $ABTS^{\bullet+}$ formation was detected by measuring UV-VIS spectra of the radical maximum at 414 nm [58]. The same conditions was used to quantify the H_2O_2 in the SPα-SOX reaction samples. In order to investigate the H_2O_2 consumption in presence of fatty acids, 1 µM SPα-SOX was incubated in 50 mM KPI at pH 7.4 with 0.5, 1, 5 or 10 mM H_2O_2 and, respectively, 0.5, 1, 5 or 10 mM lauric acid, aliquots of reaction was taken 5, 30, and 60 minutes after reaction start and diluted, when needed, 10 or 100 folds in KPI before being mixed with HRP and ABTS. In order to investigate the H_2O_2 accumulated during the SPα-SOX sarcosine-driven catalysis, 1 µM of enzyme was incubated in 50 mM KPI at pH 7.4 with 500 mM sarcosine and, 0.5, 1, 5 or 10 mM lauric acid or without lauric acid, aliquots of reaction were taken 5, 30, and 60 minutes after the reaction start and diluted, when needed, 10, 100 or 1000 folds in KPI before being mixed with HRP and ABTS.

Author contributions

DG, GG, and GC designed the experiments; DG, GC and DC performed the experiments; DG,

DC, GC, GDN, CB, MP and GG analyzed the data; DG wrote the paper. All authors reviewed and approved this article.

Acknowledgements

The plasmid containing CYP152B1 was kindly provided by Prof. Osami Shoji, Nagoya, University, Japan. This project was sponsored by the Fondazione CARIPLO (Milano, IT), project nr. 2018-2781.

Conflicts of interest

The authors declare that there is no conflict of interest.

References

1. Petek B, Marinšek Logar R (2021) Management of waste sheep wool as valuable organic substrate in European Union countries. J. Mater. Cycles Waste Manag. 23:44–54.

2. Schlossman ML, McCarthy JP (1978) Lanolin and its derivatives. J. Am. Oil Chem. Soc. 55:447–450.

3. Bertolini V, Pallavicini M, Tibhe G, Roda G, Arnoldi S, Monguzzi L, Zoccola M, Di Nardo G, Gilardi G, Bolchi C (2021) Synthesis of α-Hydroxy Fatty Acids from Fatty Acids by Intermediate α-Chlorination with TCCA under Solvent-Free Conditions: A Way to Valorization of Waste Fat Biomasses. ACS Omega 6:31901–31906.

4. Hou CT Biotransformation of unsaturated fatty acids to industrial products. In: Advances in Applied Microbiology. Vol. 47. Academic Press; 2000. pp. 201–220. Available from: https://www.sciencedirect.com/science/article/pii/S006521640047005X

5. Joo Y-C, Oh D-K (2012) Lipoxygenases: Potential starting biocatalysts for the synthesis of signaling compounds. Biotechnol. Adv. 30:1524–1532.

6. Kim K-R, Oh D-K (2013) Production of hydroxy fatty acids by microbial fatty acid-hydroxylation enzymes. Biotechnol. Adv. 31:1473–1485.

7. Bernhardt R, Urlacher VB (2014) Cytochromes P450 as promising catalysts for biotechnological application: chances and limitations. Appl. Microbiol. Biotechnol. 98:6185–6203.

8. Coon MJ (2005) Cytochrome P450: nature's most versatile biological catalyst. Annu. Rev. Pharmacol. Toxicol. 45:1–25.

9. Nelson DR (2018) Cytochrome P450 diversity in the tree of life. Biochim. Biophys. Acta BBA - Proteins Proteomics 1866:141–154.

10. Urlacher VB, Girhard M (2019) Cytochrome P450 Monooxygenases in Biotechnology and Synthetic Biology. Trends Biotechnol. 37:882–897.

11. Di Nardo G, Gilardi G (2020) Natural Compounds as Pharmaceuticals: The Key Role of Cytochromes P450 Reactivity. Trends Biochem. Sci. 45:511–525.

12. Capdevila JH, Wei S, Helvig C, Falck JR, Belosludtsev Y, Truan G, Graham-Lorence SE, Peterson JA (1996) The highly stereoselective oxidation of polyunsaturated fatty acids by cytochrome P450BM-3. J. Biol. Chem. 271:22663–22671.

13. Isin EM, Guengerich FP (2007) Complex reactions catalyzed by cytochrome P450 enzymes. Biochim. Biophys. Acta 1770:314–329.

14. Oliw EH, Bylund J, Herman C (1996) Bisallylic hydroxylation and epoxidation of polyunsaturated fatty acids by cytochrome P450. Lipids 31:1003–1021.

15. Hannemann F, Bichet A, Ewen KM, Bernhardt R (2007) Cytochrome P450 systems--biological variations of electron transport chains. Biochim. Biophys. Acta 1770:330–344.

16. Munro AW, Girvan HM, McLean KJ (2007) Variations on a (t)heme--novel mechanisms, redox partners and catalytic functions in the cytochrome P450 superfamily. Nat. Prod. Rep. 24:585–609.

17. Finnigan JD, Young C, Cook DJ, Charnock SJ, Black GW (2020) Cytochromes P450 (P450s): A review of the class system with a focus on prokaryotic P450s. Adv. Protein Chem. Struct. Biol. 122:289–320.

18. Cook DJ, Finnigan JD, Cook K, Black GW, Charnock SJ (2016) Cytochromes P450: History, Classes, Catalytic Mechanism, and Industrial Application. Adv. Protein Chem. Struct. Biol. 105:105–126.

19. Pickl M, Kurakin S, Cantú Reinhard FG, Schmid P, Pöcheim A, Winkler CK, Kroutil W, de Visser SP, Faber K (2019) Mechanistic Studies of Fatty Acid Activation by CYP152 Peroxygenases Reveal Unexpected Desaturase Activity. ACS Catal. 9:565–577.

20. Cantú Reinhard FG, Lin Y-T, Stańczak A, de Visser SP (2020) Bioengineering of Cytochrome P450 OleTJE: How Does Substrate Positioning Affect the Product Distributions? Molecules 25:2675.

21. Lin Y-T, de Visser SP (2021) Product Distributions of Cytochrome P450 OleTJE with Phenyl-Substituted Fatty Acids: A Computational Study. Int. J. Mol. Sci. 22:7172.

22. Munro AW, McLean KJ, Grant JL, Makris TM (2018) Structure and function of the cytochrome P450 peroxygenase enzymes. Biochem. Soc. Trans. 46:183–196.

23. Jiang Y, Peng W, Li Z, You C, Zhao Y, Tang D, Wang B, Li S (2021) Unexpected Reactions of α,β-Unsaturated Fatty Acids Provide Insight into the Mechanisms of CYP152 Peroxygenases. Angew. Chem. Int. Ed. 60:24694–24701.

24. Shoji O, Fujishiro T, Nishio K, Kano Y, Kimoto H, Chien S-C, Onoda H, Muramatsu A, Tanaka S, Hori A, et al. (2016) A substrate-binding-state mimic of H 2 O 2 -dependent cytochrome P450 produced by one-point mutagenesis and peroxygenation of non-native substrates. Catal. Sci. Technol. 6:5806–5811.

25. Fujishiro T, Shoji O, Nagano S, Sugimoto H, Shiro Y, Watanabe Y (2011) Crystal Structure of H2O2-dependent Cytochrome P450SPα with Its Bound Fatty Acid Substrate. J. Biol. Chem. 286:29941–29950.

26. Matsunaga I, Sumimoto T, Ueda A, Kusunose E, Ichihara K (2000) Fatty acid-specific, regiospecific, and stereospecific hydroxylation by cytochrome P450 (CYP152B1) from Sphingomonas paucimobilis: Substrate structure required for α-hydroxylation. Lipids 35:365–371.

27. Matsunaga I, Yokotani N, Gotoh O, Kusunose E, Yamada M, Ichihara K (1997) Molecular cloning and expression of fatty acid alpha-hydroxylase from Sphingomonas paucimobilis. J. Biol. Chem. 272:23592–23596.

28. Ezraty B, Gennaris A, Barras F, Collet J-F (2017) Oxidative stress, protein damage and repair in bacteria. Nat. Rev. Microbiol. 15:385–396.

29. Paul CE, Churakova E, Maurits E, Girhard M, Urlacher VB, Hollmann F (2014) In situ formation of H2O2

for P450 peroxygenases. Bioorg. Med. Chem. 22:5692–5696.

30. Gomez de Santos P, Lazaro S, Viña-Gonzalez J, Hoang MD, Sánchez-Moreno I, Glieder A, Hollmann F, Alcalde M (2020) Evolved Peroxygenase–Aryl Alcohol Oxidase Fusions for Self-Sufficient Oxyfunctionalization Reactions. ACS Catal. 10:13524–13534.

31. Gilardi G, Meharenna YT, Tsotsou GE, Sadeghi SJ, Fairhead M, Giannini S (2002) Molecular Lego: design of molecular assemblies of P450 enzymes for nanobiotechnology. Biosens. Bioelectron. 17:133–145.

32. Sadeghi SJ, Gilardi G (2013) Chimeric P450 enzymes: activity of artificial redox fusions driven by different reductases for biotechnological applications. Biotechnol. Appl. Biochem. 60:102–110.

33. Chlumsky LJ, Zhang L, Jorns MS (1995) Sequence Analysis of Sarcosine Oxidase and Nearby Genes Reveals Homologies with Key Enzymes of Folate One-carbon Metabolism *. J. Biol. Chem. 270:18252–18259.

34. Wagner MA, Khanna P, Jorns MS (1999) Structure of the Flavocoenzyme of Two Homologous Amine Oxidases: Monomeric Sarcosine Oxidase and N-Methyltryptophan Oxidase. Biochemistry 38:5588–5595.

35. Wagner MA, Trickey P, Chen ZW, Mathews FS, Jorns MS (2000) Monomeric sarcosine oxidase: 1. Flavin reactivity and active site binding determinants. Biochemistry 39:8813–8824.

36. Wagner MA, Jorns MS (2000) Monomeric sarcosine oxidase: 2. Kinetic studies with sarcosine, alternate substrates, and a substrate analogue. Biochemistry 39:8825–8829.

37. Trickey P, Wagner MA, Jorns MS, Mathews FS Monomeric sarcosine oxidase: structure of a covalently flavinylated amine oxidizing enzyme. :15.

38. Motiuk K (1979) Wool wax acids: A review. J. Am. Oil Chem. Soc. 56:91–97.

39. Moldovan Z, Jover E, Bayona JM (2002) Gas chromatographic and mass spectrometric methods for the characterisation of long-chain fatty acids: Application to wool wax extracts. Anal. Chim. Acta 465:359–378.

40. Nelson DR (2005) Cytochrome P450: Structure, Mechanism, and Biochemistry, 3rd ed Edited by Paul R. Ortiz de Montellano (University of California, San Francisco). Kluwer Academic/Plenum Publishers: New York. 2005. xx + 690 pp. $149.00. ISBN 0-306-48324-6. J. Am. Chem. Soc. 127:12147–12148.

41. Girvan HM, Poddar H, McLean KJ, Nelson DR, Hollywood KA, Levy CW, Leys D, Munro AW (2018) Structural and catalytic properties of the peroxygenase P450 enzyme CYP152K6 from Bacillus methanolicus. J. Inorg. Biochem. 188:18–28.

42. Belcher J, McLean KJ, Matthews S, Woodward LS, Fisher K, Rigby SEJ, Nelson DR, Potts D, Baynham MT, Parker DA, et al. (2014) Structure and Biochemical Properties of the Alkene Producing Cytochrome P450 OleTJE (CYP152L1) from the Jeotgalicoccus sp. 8456 Bacterium. J. Biol. Chem. 289:6535–6550.

43. Tong Y, Xin Y, Yang H, Zhang L, Wang W (2014) Efficient improvement on stability of sarcosine oxidase via poly-lysine modification on enzyme surface. Int. J. Biol. Macromol. 67:140–146.

44. Xin Y, Zheng M, Wang Q, Lu L, Zhang L, Tong Y, Wang W (2016) Structural and catalytic alteration of sarcosine oxidase through reconstruction with coenzyme-like ligands. J. Mol. Catal. B Enzym. 133:S250–S258.

45. Albertolle ME, Kim D, Nagy LD, Yun C-H, Pozzi A, Savas Ü, Johnson EF, Guengerich FP (2017) Heme–thiolate sulfenylation of human cytochrome P450 4A11 functions as a redox switch for catalytic inhibition. J. Biol. Chem. 292:11230–11242.

46. Matthews S, Tee KL, Rattray NJ, McLean KJ, Leys D, Parker DA, Blankley RT, Munro AW (2017) Production of alkenes and novel secondary products by P450 OleTJE using novel H2O2-generating fusion protein systems. FEBS Lett. 591:737–750.

47. Ciaramella A, Catucci G, Di Nardo G, Sadeghi SJ, Gilardi G (2020) Peroxide-driven catalysis of the heme domain of A. radioresistens cytochrome P450 116B5 for sustainable aromatic rings oxidation and drug metabolites production. New Biotechnol. 54:71–79.

48. Omura T, Sato R (1964) The Carbon Monoxide-binding Pigment of Liver Microsomes: II. SOLUBILIZATION, PURIFICATION, AND PROPERTIES. J. Biol. Chem. 239:2379–2385.

49. Farber P, Darmawan H, Sprules T, Mittermaier A (2010) Analyzing protein folding cooperativity by differential scanning calorimetry and NMR spectroscopy. J. Am. Chem. Soc.

50. Matsunaga I, Kusunose E, Yano I, Ichihara K (1994) Separation and partial characterization of soluble fatty acid alpha-hydroxylase from Sphingomonas paucimobilus. Biochem. Biophys. Res. Commun. 201:1554–1560.

51. Catucci G, Ciaramella A, Di Nardo G, Zhang C, Castrignanò S, Gilardi G (2022) Molecular Lego of Human Cytochrome P450: The Key Role of Heme Domain Flexibility for the Activity of the Chimeric Proteins. Int. J. Mol. Sci. 23:3618.

52. Sadeghi SJ, Meharenna YT, Fantuzzi A, Valetti F, Gilardi G (2000) Engineering artificial redox chains by molecular “Lego.” Faraday Discuss.:135–153; discussion 171-190.

53. Santoro MM, Liu Y, Khan SM, Hou LX, Bolen DW (1992) Increased thermal stability of proteins in the presence of naturally occurring osmolytes. Biochemistry 31:5278–5283.

54. Kumar R (2009) Role of naturally occurring osmolytes in protein folding and stability. Arch. Biochem. Biophys. 491:1–6.

55. Omura T, Sato R (1964) The Carbon Monoxide-binding Pigment of Liver Microsomes: I. EVIDENCE FOR ITS HEMOPROTEIN NATURE. J. Biol. Chem. 239:2370–2378.

56. Catucci G, Aramini D, Sadeghi SJ, Gilardi G (2020) Ligand stabilization and effect on unfolding by polymorphism in human flavin-containing monooxygenase 3. Int. J. Biol. Macromol. 162:1484–1493.

57. Gao C, Catucci G, Castrignanò S, Gilardi G, Sadeghi SJ (2017) Inactivation mechanism of N61S mutant of human FMO3 towards trimethylamine. Sci. Rep. 7:14668.

58. Kadnikova EN, Kostić NM (2002) Oxidation of ABTS by hydrogen peroxide catalyzed by horseradish peroxidase encapsulated into sol–gel glass.: Effects of glass matrix on reactivity. J. Mol. Catal. B Enzym. 18:39–48.

Tables

Table 1. Hydrogen peroxide tolerance of the fusion protein heme domain. Decay rate constants for heme oxidation (k) and associated Soret peak absorption change amplitudes (A) for SPα-SOX (417 nm) over 1 hour incubation in presence of 1 mM H_2O_2. Data are compared to (k) and (A) reported for $OleT_{JE}$, CYP51B1, P450 BM3, CYP121A1 [46] and CYP116B5 [47].

	H_2O_2 concentration	**k (min^{-1})**	**A**
SPα-SOX	1 mM	0.0021 ± 0.000055	0.018 ± 0.001
OleTJE[46]	1 mM	6.99 ± 0.16	0.065 ± 0.001
CYP51B1[46]	1 mM	22.15 ± 0.17	0.28 ± 0.002
BM3[46]	1 mM	13.84 ± 0.15	0.23 ± 0.009
CYP121A1[46]	1 mM	16.29 ± 0.18	0.19 ± 0.001
CYP116B5[47]	2 mM	0.144	0.022 ± 0.006

Table 2. Conversion of the three lanoline-representative fatty acids by SPα-SOX using two different H_2O_2 supply system. The H_2O_2 concentration used was equal to that of the fatty acid (0.5 , 1 , 5 , 10 mM respectively). The sarcosine concentration used was 500 mM. 1 μM SPα-SOX was used in all the experiments. Data are compared to the % of conversion and TON of lauric acid reported using the isolated $P450_{SPα}$ and the same reaction condition [23].

		SPα-SOX				$P450_{SPα}$ [23]	
Substrate	**Concentration**	**H_2O_2**		**Sarcosine**		**H_2O_2**	
		% conversion	**TON**	**% conversion**	**TON**	**% conversion**	**TON**
Lauric Acid (C12)	0.5 mM	100	500	100	500	63.4	317
	1 mM	100	1000	100	1000	53.4	534
	5 mM	85.5	4275	87.6	4380	66.7	3336
	10 mM	73.6	7359	68.0	6800	23.1	2307
Myristic Acid (C14)	0.5 mM	56.2	281	100.0	500	n/a	
	1 mM	78.4	784	100.0	1000	n/a	
	5 mM	86.9	4345	94.3	4715	n/a	
	10 mM	35.6	3560	67.5	6750	n/a	
Parmitic Acid (C16)	0.5 mM	71.3	357	77.6	388	n/a	
	1 mM	65.9	659	80.2	802	n/a	
	5 mM	83.7	4185	20.4	1021	n/a	
	10 mM	70.9	7090	19.6	1962	n/a	

Figures

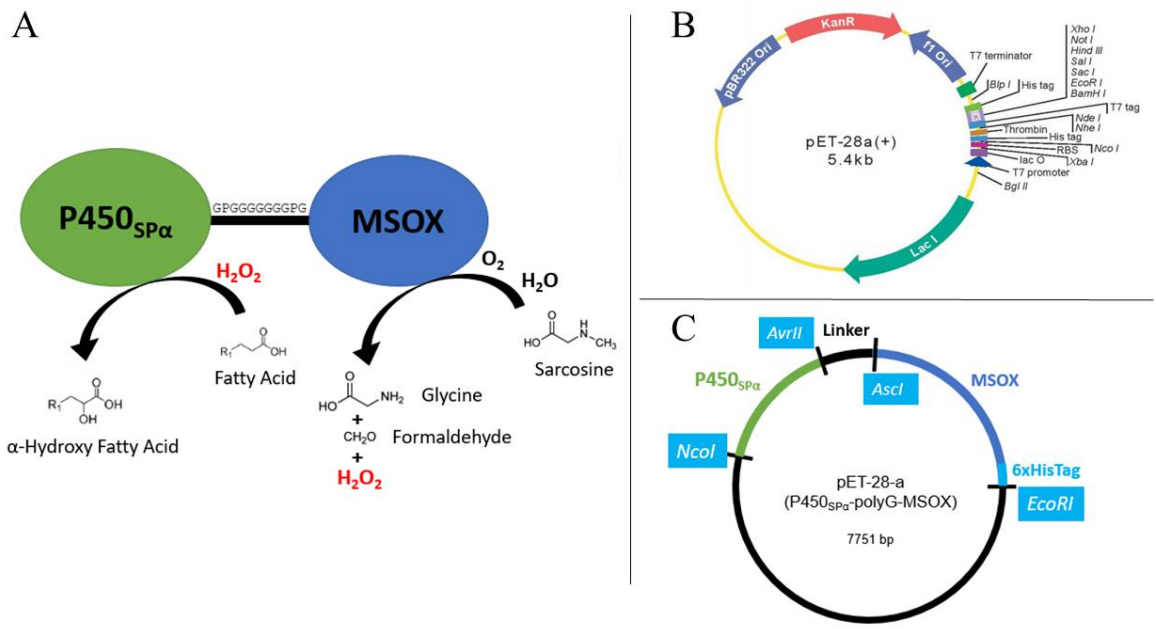

Fig. 1

Figure 1. (A) Schematic representation of SPα-SOX construct. The fusion enzyme exploits the *Bacillus sp. B-0618* MSOX catalysis to oxidize sarcosine (N-methylglycine) to yield glycine, formaldehyde, and hydrogen peroxide as by-product. *Sphingomonas paucimobilis* $P450_{SP\alpha}$ uses hydrogen peroxide to catalyse the conversion of fatty acids to α-hydroxy fatty acids. (B) pET-28a(+) plasmid map containing f1 and pBR322 origin of replication, KanR conferring resistence to kanamycin, T7 promoter, T7 terminator and several restriction sites; some restriction sites were lost after cloning. (C) Schematic representation of SPα-SOX gene into the pET-28-a(+) expression vector with highlighted restriction sites and 6xHisTag.

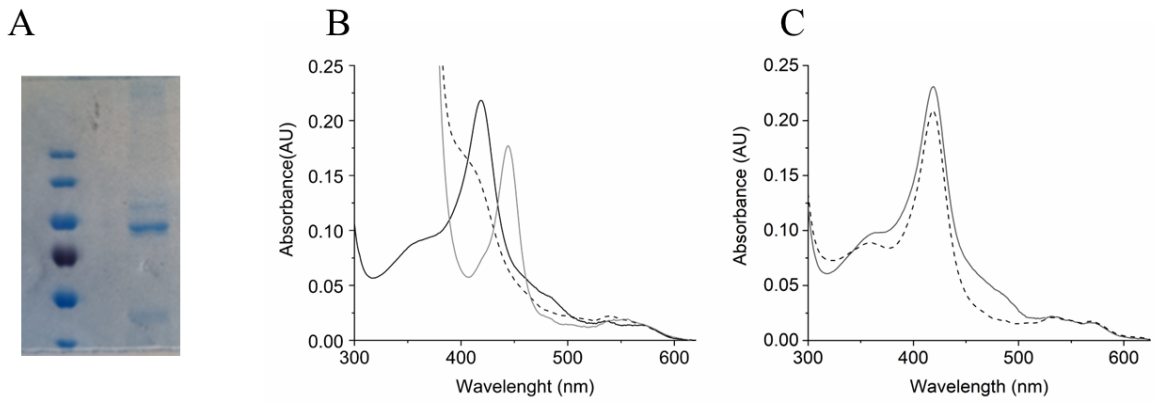

Fig. 2

Figure 2. Characterization of the purified SPα-SOX. (A) SDS-PAGE of SPα-SOX purified by IMAC and SEC (protein ladder MW: 180, 130, 100, 70, 55, 40). (B) Formation of the CO-form of $P450_{Spα}$. UV-visible spectra of SPα-SOX in the oxidized form (black solid line), reduced form after sodium dithionite addition (black dashed line) and CO-complex after CO bubbling (gray solid line). (C) UV-visible spectra of SPα-SOX before (black solid line) and after (black dashed line) the addition of sarcosine. Spectra show the bleaching of absorbance at λ_{372} and λ_{454} due to MSOX reduction.

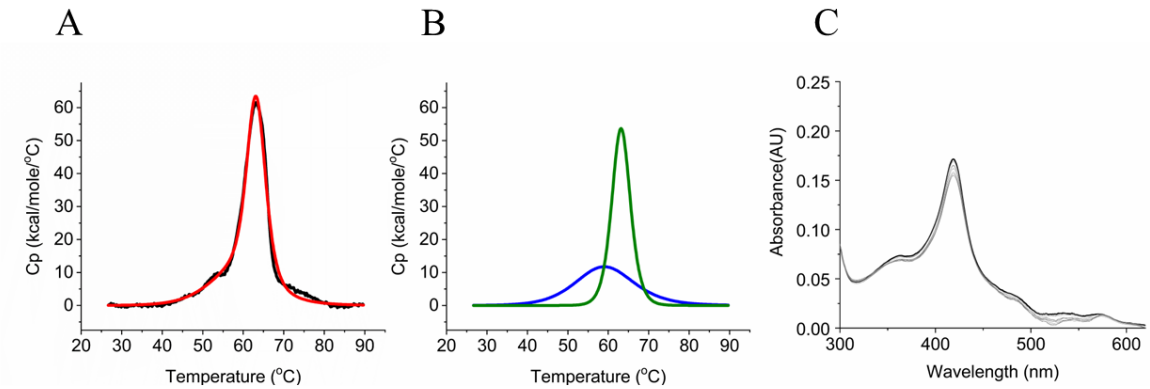

Fig. 3

Figure 3. Thermal denaturation and H_2O_2-tolerance of SPα-SOX. Panel A and B show the DSC measurements, carried out at scan/rate of 60 °C/h. (A) The experimental curve (black line) and fitting of the experimental curve applying a non-two-state denaturation model (red line). (B) The deconvolution of the first peak (blue line) and of the second peak (orange line). (C) UV-visible spectra of SPα-SOX heme domain, before (thick solid line) and after the addition of 1 mM H_2O_2. Proteins is at concentration of 1.7 μM. Spectra show $P450_{SPa}$ absorbance decrease due to H_2O_2-mediated oxidation of the prosthetic group, data were recorded every 1.5 minutes over 1 h.

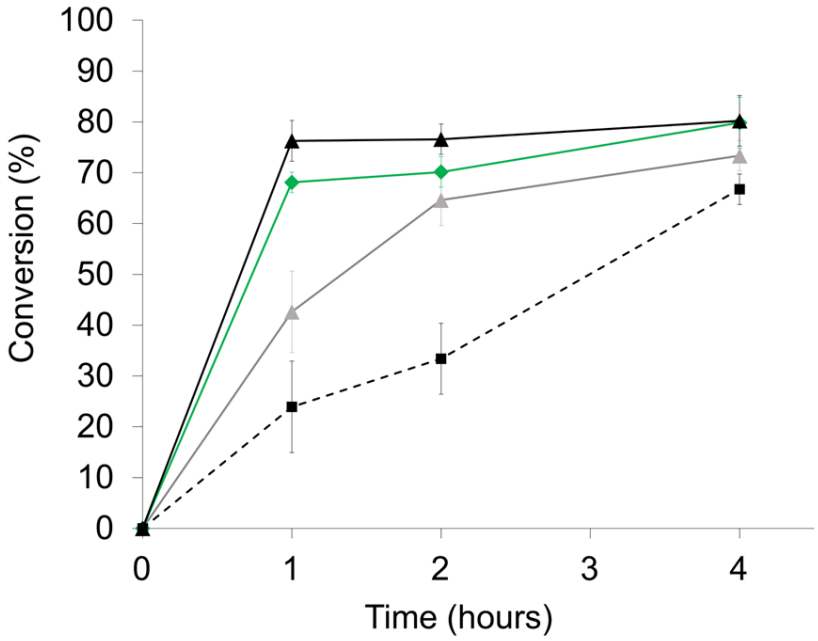

Fig. 4

Figure 4. Time dependence of palmitic acid conversion catalyzed by SPα-SOX self-sufficient at different concentration of sarcosine. The reaction was performed at 30° C using 1 μM SPα-SOX, 1 mM palmitic acid and 25 mM (grey triangles, gray solid line), 250 mM (green rhombs, green solid line), 500 mM (black triangles, black solid line) or 1 M (black squares, black dashed line) of sarcosine.

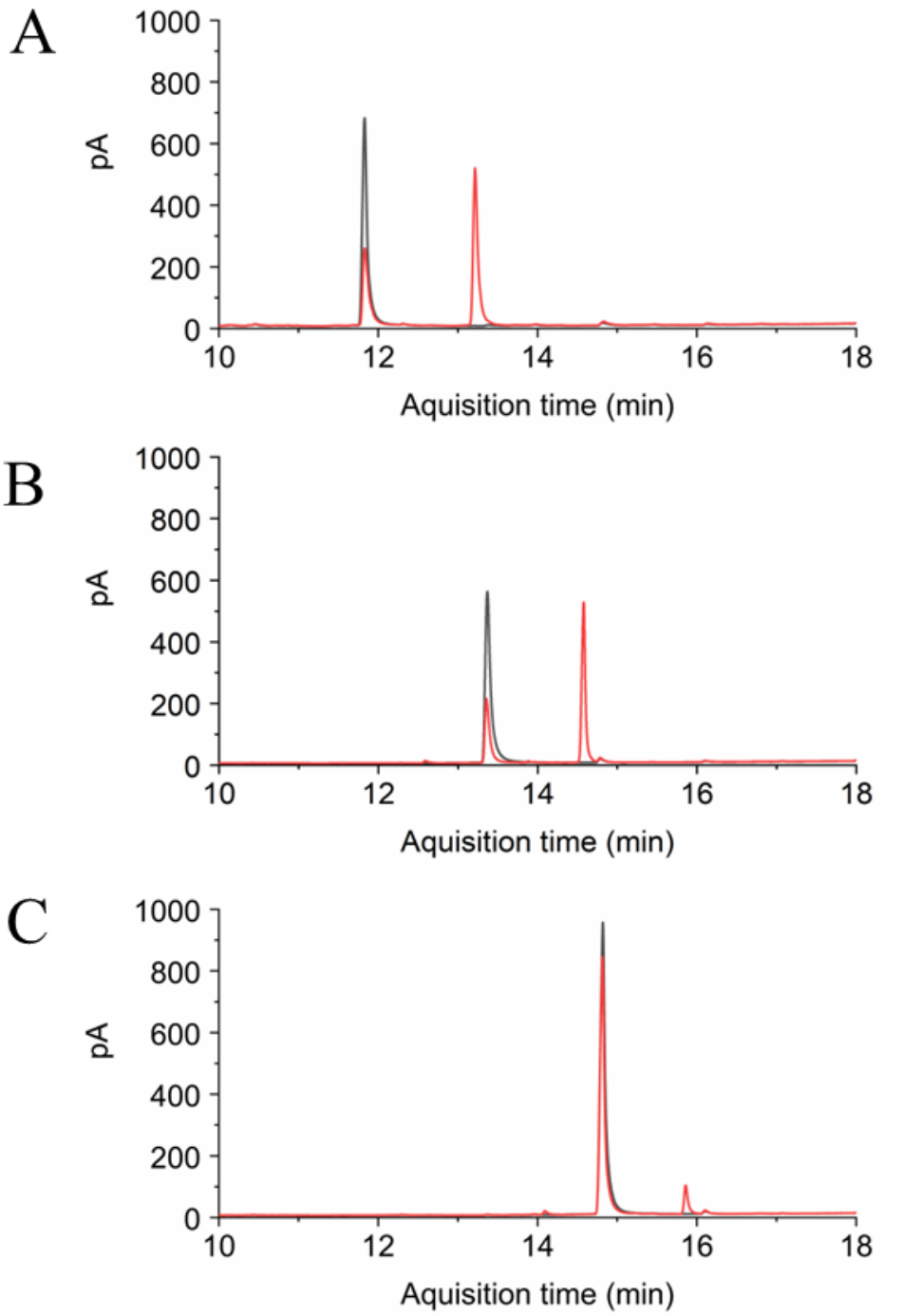

Fig. 5

Figure 5. Gas chromatography traces showing the product formed by the SPα-SOX reaction of conversion of lauric acid (A), myristic acid (B) and palmitic acid (C). Reaction were carried out over 6 hours at 30°C using 1 µM SPα-SOX, 10 mM fatty acid and 500 mM sarcosine. Red lines are the reaction samples, black lines are samples containing identical mixtures without

the enzyme.

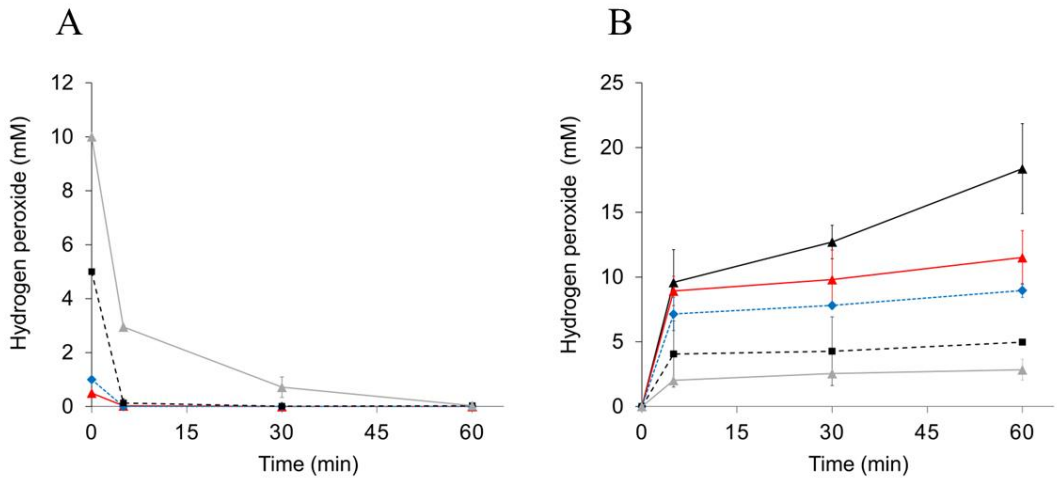

Fig. 6

Figure 6. (A) Time dependence of H_2O_2 consumption by SPα-SOX catalysis. H_2O_2 concentration used was equal to that of the lauric acid, i.e. 0.5 mM (red triangles, red solid line), 1 mM (blue rhombs, blue dashed line) , 5 mM (black squares, black dashed line), 10 mM (gray triangles, gray solid line). (B) H_2O_2 time course of accumulation catalyzed by SPα-SOX in presence of 500 mM sarcosine and lauric acid at 0.5 mM (red triangles, red solid line), 1 mM (blue rhombs, blue dashed line), 5 mM (black squares, black dashed line), 10 mM (gray triangles, gray solid line) or without lauric acid (black triangles, black solid line)